Magnetism in Cool Evolved Stars: the M giants EK Bootis and β Pegasi

S. Georgiev[1,2], R. Konstantinova-Antova[1], A. Lèbre[2], M. Aurière[3], C. Charbonnel[3,4], A. Palacios[2], N. Drake[5,6,7], R. Bogdanovski[1]

[1] Institute of Astronomy and NAO, Bulgarian Academy of Science, 1784 Sofia, Bulgaria

[2] LUPM, UMR 5299, Université de Montpellier, CNRS, place Eugène Bataillon, 34095 Montpellier, France

[3] Université de Toulouse, Institut de Recherche en Astrophysique et Planétologie, 14 avenue Édouard Belin, 31400 Toulouse, France

[4] Department of Astronomy, University of Geneva, Chemin des Maillettes 51, 1290 Versoix, Switzerland

[5] Laboratory of Observational Astrophysics, Saint Petersburg State University, Universitetski pr. 28, Petrodvoretz 198504, Saint Petersburg, Russia

[6] Observatório Nacional/MCTIC, Rua Gen. José Cristino, 77, 20921-400, Rio de Janeiro, Brazil

[7] Laboratório Nacional de Astrofísica/MCTIC, Rua dos Estados Unidos 154, 37504-364, Itajubá , Brazil

sgeorgiev@astro.bas.bg

(Submitted on 04.11.2019. Accepted on 18.02.2020)

Abstract. We present a long-term spectropolarimetric study of the active M giants EK Bootis (M5III) and β Pegasi (M2.5II-III). For each star, the variability of the disk-averaged longitudinal component of the magnetic field (B_l) is shown, along with the behavior of different spectral activity indicators. The possible nature of the secondary component of EK Boo is discussed. We compare the observed variations in the activity proxies of each of the two giants and discuss possible physical explanations for the structure of their respective magnetic fields. For both objects, observations in linear polarisation are also presented and briefly discussed.

1. Introduction

Magnetism in cool evolved stars has been extensively studied in the case of G- and K giants (see Konstantinova-Antova et al. 2013; Aurière et al. 2015). Aurière et al. (2015) studied 48 such giants and magnetism was detected in 29 of them. A correlation between the magnetic field strength and the Rossby number in the magnetically detected stars was determined, favoring the operation of an $\alpha - \omega$ dynamo. The positions of these magnetic giants in the Hertzsprung-Russell diagram (HRD) define two so-called "magnetic strips" that correspond to specific evolutionary stages: 1) around the first dredge-up at the base of the Red Giant Branch (RGB) and during the core-helium burning and 2) at the tip of the RGB and early Asymptotic Giant Branch (AGB) stage. Based on observational results, a theoretical framework was built by Charbonnel et al. (2017) to explain the existence of surface magnetic fields in these stars. In the samples of M giants, studied by Konstantinova-Antova et al. (2010; 2013; 2014), more than 60% of the stars are magnetically active. However, recent results (Konstantinova-Antova et al. 2018; 2019, in prep.) do not favor the $\alpha - \omega$ dynamo to explain the magnetic field in these stars. Here we present a further study of magnetism in two M giants, EK Boo and β Peg.

2. Data and methods

2.1. Observations and data reduction

The M giants EK Boo and β Peg were observed using the instrument Narval mounted on the 2m Telescope Bernard-Lyot (TBL) at the Pic du Midi observatory, France. Narval is a high-resolution fiber-fed echelle spectropolarimeter (Aurière 2003). This instrument works in the spectral range of 375 – 1050 nm and has a resolving power of 65000. It allows simultaneous measurement of the full intensity as a function of wavelength (Stokes I) and the intensity in linear (Stokes U or Q) or circular (Stokes V) polarisation versus wavelength. Narval is capable of detecting polarisation within individual lines with an accuracy of about $10^{-4}I_c$ (I_c being the intensity of the unpolarised continuum).
We used Narval for observations in circular polarisation to search for Zeeman signatures in the Stokes V profiles, indicative of the presence of a magnetic field. Some observations in linear polarisation were also obtained. All data were treated initially by the automatic reduction software LibreEsprit (Donati et al. 1997), which performs optimal spectrum extraction, wavelength calibration, heliocentric frame correction and continuum normalization.

2.2. Data analysis

Having obtained reduced by LibreEsprit data, we used the Least Square Deconvolution (LSD) method (Donati et al. 1997), which averages the profiles of more than ten thousand spectral lines (≈15000 in the cases of EK Boo and β Peg) to generate a mean line profile, both in Stokes I and in polarised light. In this way, the detection of weak polarised structures associated with spectral lines, and resulting from magnetic fields of low intensity, becomes possible. The method also gives a diagnostic null spectrum which should not present any feature. Its purpose is to diagnose the presence of spurious contributions to the Stokes $V/U/Q$ spectrum. To perform the LSD method we used line masks constructed from the VALD database (Kupka et al. 1999) with the following parameters: $T_{\rm eff}$=3500 K, log$g$=0.5, microturbulence of 2.0 km/s for EK Boo and $T_{\rm eff}$=3700 K, log$g$=1.0, microturbulence of 2.0 km/s for β Peg. Both masks are calculated for solar abundances.

The method has a built-in procedure for statistical evaluation of the signal detection probability. According to this procedure, we can have a definite detection of polarisation, a marginal detection, or a non-detection (DD, MD and ND, respectively). The procedure is based on a reduced χ^2 test and yields a DD if the false alarm probability is smaller than 10^{-5}, MD if it is larger than 10^{-5}, but smaller than 10^{-3}, and ND otherwise.

2.3. Measurements of magnetic field strength and activity indicators

Using the Stokes V data, we calculated the line-of-sight component of the magnetic field (B_l) using the first-order moment method (Rees & Semel 1979; Donati et al. 1997); the typical error in the B_l calculations is 0.7 G for EK Boo and 0.3 G for β Peg. Using the Stokes I data, we measured the intensity of the spectral activity indicators CaII H&K, Hα and CaIRT by calculating the S-index, defined in the Mount Wilson survey (Duncan et al. 1991) and the related Hα and CaIRT indices. By fitting the mean Stokes I profiles with a gaussian, we also calculated the stellar radial velocity $V_{\rm rad}$. The radial velocity bin in the LSD ouput is 1.8 km/s, and following the Nyquist theorem, we estimate an error of 0.9 km/s for our $V_{\rm rad}$ measurements.

Due to a technical problem with Narval in the summers of 2011 and 2012 (one of the spectropolarimeter's Fresnel rhombs was out of position, hence giving false Stokes V data), we could not obtain reliable B_l measurements for these periods. However, the unpolarised spectra were not affected, allowing the measurement of the spectral activity indicators and the $V_{\rm rad}$.

The results for both stars are described in the following two sections.

3. EK Boo

3.1. General characteristics

EK Boo (HD 130144) is a M5III semiregular variable giant star (Samus et al. 2017) of visual magnitude $V = 5.63^m$ (Ducati 2002). This star has an X-ray luminosity $L_{\rm X} > 10^{30}$ erg s^{-1} (Hünsch et al. 1998), which is unusually high for this spectral type. EK Boo has a projected rotational velocity $v{\rm sin}i = 8.5 \pm 0.5$ km/s and it is the first apparently single M giant for which a direct detection of a surface magnetic field was reported (Konstantinova-Antova et al. 2010).

3.2. Magnetic field strength, spectral activity indicators and radial velocity

We obtained 51 Stokes V observations of EK Boo between April 2008 and April 2019, of which only 18 show detections. The log of observations is shown in Table 1 in the Appendix. Typical signal-to-noise ratios (SNR) of the spectra peak at about 1200. The mean Stokes V profiles of EK Boo, constructed with the LSD method, show strong variability both at long- and short-term timescales. A sample of the LSD results are presented in Figure 1, showing the LSD profiles for the dates March 31 2011 (ND), April 7 2011 (DD) and April 30 2011 (ND). In this plot we see the mean Stokes V profile changing considerably in the course of a single month, while the accuracy

of the measurements for these observations does not vary considerably. Measured values of the B_l, spectral activity indicators and radial velocities are presented in Figure 2. The longitudinal component of the magnetic field varies on both long and short time scales: observations for which we have a definite detection of mean Stokes V signatures are followed shortly by observations with no detection. The B_l varies in the range of -10.20 ± 0.86 G to 4.93 ± 0.71 G.

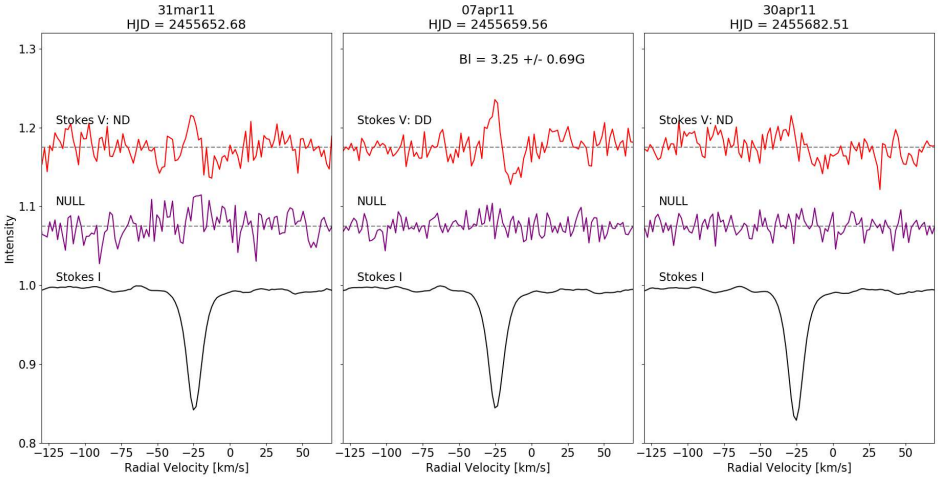

Fig. 1. Example of LSD results from EK Boo observations. The Stokes V and NULL signals are shifted vertically and multiplied by a factor of 10^3 for display purposes. The result of the statistical test is indicated for each observation and the B_l value is given for the detections.

The magnetic field is a vector, and we can only measure its line-of-sight component integrated over the whole visible stellar hemisphere, B_l. The individual magnetic structures contribute to the B_l with different signs depending on their polarity: structures of opposing polarities would cancel each other out in their contribution to the line-of-sight component. On the other hand, the spectral proxies trace the magnetic heating in the stellar atmosphere. Their variability depends on the integrated heating by the magnetic structures, regardless of their polarity. In EK Boo, the spectral activity indicators show a complex behavior with respect to the B_l. No clear correlation is observed. This suggests that the field is not of simple geometry: instead, it seems that small-scale magnetic structures contribute to the magnetic heating of the stellar atmosphere. Because of the relatively low $v\sin i$ however, we cannot resolve fine details on the stellar disc.

In Figure 2, a long-term variability of the B_l and the activity indicators is obvious. In the first half of our dataset, between April 2008 and August 2013 (HJD 2454562 to 2456516) the B_l as well as the spectral activity indicators vary more than in the second half of the dataset, where they display a more steady behavior. Also, before August 2013 we report more detections

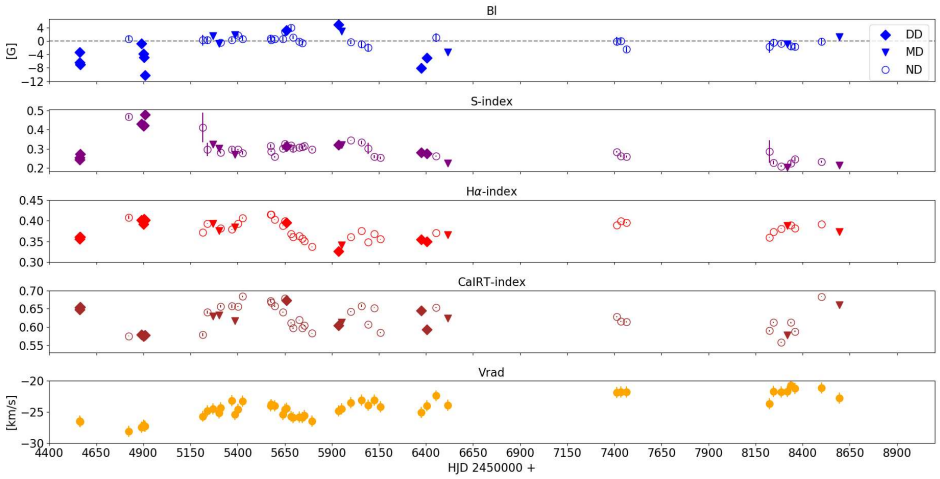

Fig. 2. Magnetic field, spectral activity indicators and radial velocity measurements of EK Boo. The different symbols denote the type of detection of circular polarisation.

of magnetic field, while between January 2016 and April 2019 (HJD 2457413 to 2458594) we have only two marginal detections. The recent behavior of the magnetic field strength and spectral indicators might be indicative that the magnetic activity of EK Boo declines in the second half of the dataset with respect to the level in the first half. However, taking into account the smaller number of observations during the last observational seasons, we cannot have a firm conclusion on it.

Within the timescale of one month (March 2009, April 2011) we observe fast variability of the magnetic field, which indicates dynamics in the magnetic structures. Looking at the activity indicators, however, we do not find evidence of flares. This means that the magnetic variability in EK Boo is rather different than that in the G and K giants studied in detail, e.g. V390 Aur (Konstantinova-Antova et al. 2012), OU And (Borisova et al. 2016), β Cet (Tsvetkova et al. 2019), OP And (Georgiev et al. 2018). Such vigorous dynamics might be associated with changes in the convective structure as a tracer of the magnetic field. Whether an $\alpha - \omega$ or another kind of dynamo is operating in such conditions is a subject of a further study.

The behavior of the radial velocity of EK Boo is interesting, as can be seen in Figure 2. At the beginning of our dataset, on April 4 2008 (HJD = 2454562) we have $V_{\rm rad} = -26.5 \pm 0.9$ km/s, after which the value steadily grows over time and our last observation, done on April 19 2019, yields $V_{\rm rad} = -22.8 \pm 0.9$ km/s. A long-term trend in the radial velocity is apparent, suggesting the existence of a companion. The secondary component must be much fainter than the primary star, since we observe no spectral indications of binarity. This excludes the possibility that the observed polarised signatures are related to the secondary component, as only a sufficiently bright object could cause a detection of polarised signal. Taking

into account the unusually high X-ray luminosity of EK Boo and the low luminosity of the companion in the visible domain, we suggest that the secondary component could be an active red dwarf, responsible for the large $L_{\rm X}$. This is in good agreement with the results of Horch et al. (2011), who sucessfuly resolve two components in EK Boo separated by 0.2023 arcseconds. According to these authors, the components differ in magnitude in the 562 nm and 692 nm filters by 3.02^m and 3.51^m respectively, meaning that the secondary component must be slightly hotter than the primary, supporting our hypothesis that it is a red dwarf.

Our dataset spans over 11 years and during this time the $V_{\rm rad}$ variation does not exhibit periodicity. This suggests that the orbital period of the system is long, meaning that the distance between the components is very large with respect to their size, i.e. we have a wide binary system. This excludes the possibility that the activity of EK Boo is caused by tidal interactions like in RS CVn variables. Indeed, considering the parallax to be 4.04 miliarcseconds (van Leeuwen 2007) and the apparent angular distance between the components of 0.2023 arcseconds (Horch et al. 2011), we find the linear separation between the two stars to be 50 AU. Assuming circular orbit and neglecting the mass of the secondary (less massive) component, we calculate the orbital period of the system to be 187 or 250 years considering the mass of the primary (more massive) equal to 3.6 $M_\odot$ or 2 $M_\odot$, respectively (Konstantinova-Antova et al. 2010).

3.3. Linear polarisation

We observed EK Boo in linear polarisation during three nights in 2019: March 15 (HJD = 2458558), April 30 (HJD = 2458604) and May 30 (HJD = 2458634). For all of them we have both Stokes U and Q measurements. We analyzed the data and found no polarisation signatures linked to individual spectral lines. We then applied the LSD method to the observations in search for a mean polarisation signal. The output is shown in Figure 3 and the results of the statistical test are indicated for each observation. The LSD method reveals a clear mean linear polarisation signal in all of our observations. A clear signature seems to always be present in Stokes U, which is not the case in Stokes Q. The appearance of signal in the LSD profiles and not in the observational spectropolarimetric data means that a mean polarisation exists in the spectra of EK Boo, but the signal within individual lines is below our detection limit.

Recent studies (Aurière et al. 2016, Mathias et al. 2018, Lòpez Ariste et al. 2018) have explained the linear polarisation observed in the cool evolved supergiant Betelgeuse with the presence of giant convective cells at the photospheric layer. Further observations of EK Boo are necessary in order to explain if the observed linear polarisation signal in EK Boo is due to surface brightness inhomogeneities (similarly to the case of Betelgeuse), or if it has some other origin.

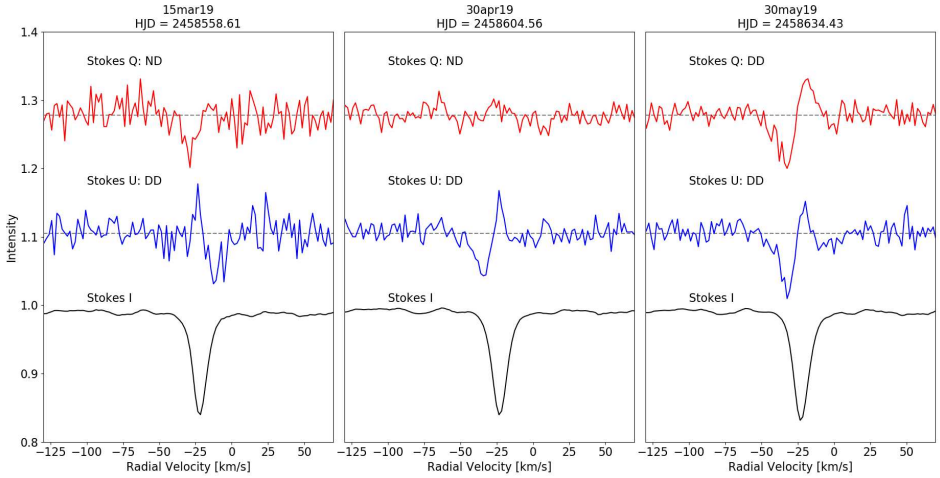

Fig. 3. LSD profiles of observations in linear polarisation of EK Boo. The Stokes $U\&Q$ signals are shifted vertically and multiplied by a factor of 10^3 for display purposes. The diagnostic null spectra are all flat and are not shown. The result of the statistical test is indicated for each observation.

4. β Peg

4.1. General characteristics

β Peg (HD 217906) is a $V = 2.4^m$ (Ducati 2002) M2.5II-III semiregular variable star with $P = 43.3d$ (Tabur et al. 2009). We estimate a value of $v\sin i = 7$ km/s for this giant. β Peg is known to be a magnetic early-AGB star (Konstantinova-Antova et al. 2014).

4.2. Magnetic field strength, spectral activity indicators and radial velocity

In the period July 2015 – January 2019 we obtained 15 observations of β Peg in circular polarisation, out of which 10 yield magnetic field detections. The typical SNR of the spectra is ≈1400. The log of observations is presented in Table 2 in the Appendix. Applying the LSD method to the observations of β Peg, we find significant variability in the mean Stokes V profiles, as well as in the value of the B_l. An example of the LSD results is given in Figure 4 and the measurements of the B_l, spectral activity indicators and radial velocities are shown in Figure 5.

Figure 5 clearly shows variability in the longitudinal component of the magnetic field, both in strength and polarity. Also, variability in the activity indicators is apparent. The S-, Hα- and CaIRT-indices seem to vary together with the magnetic field. This is especially obvious in the first half of our dataset (HJD 2457150 to 2457750), where we have the most detections. We interpret the observed correlation between the B_l and the spectral

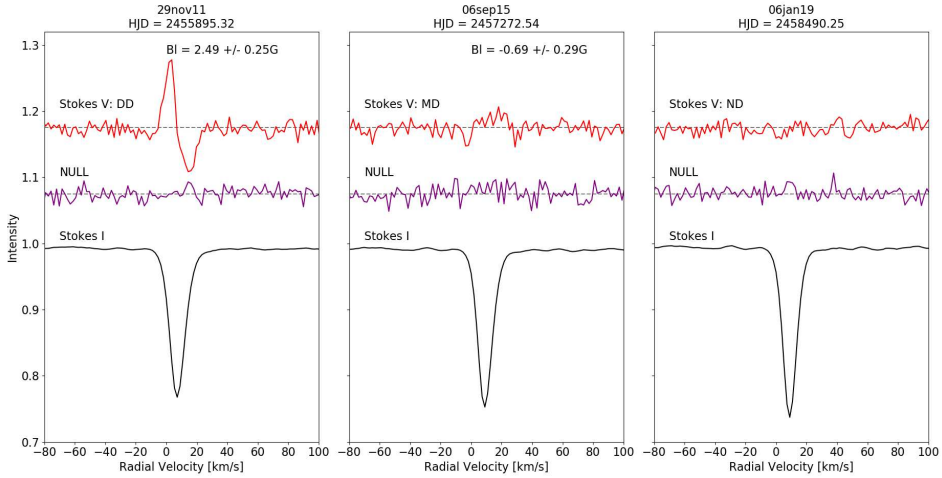

Fig. 4. Example of LSD results from β Peg observations. The result of the statistical test is indicated for each observation and the B_l value is given for the detections.

activity indicators of β Peg as an indication of a magnetic field dominated by large-scale structures. We, thus, expect the field to have a more simple poloidal geometry.

The $V_{\rm rad}$ shows some variability which could be caused by pulsations, as expected since β Peg is a semiregular variable star.

4.3. Linear polarisation

We observed β Peg in linear polarisation during two nights in 2015: July 8 (HJD = 2457212) and September 6 (HJD = 2457272). For these dates we have both Stokes U and Q measurements. No polarisation signatures were found associated to individual lines, nor to the LSD profiles.

5. Summary

The long-term variability of the active M giants EK Boo and β Peg is studied and presence of magnetic field of variable strength is observed in both objects. It is stronger in EK Boo, which also has the higher $v\sin i$ (8.5 km/s). Analysis of the behavior of the magnetic field line-of-sight component B_l together with the spectral activity indicators, the CaII H&K, Hα and CaIRT lines shows, that in the two stars the magnetic field topologies differ: in EK Boo we observe variability that could be associated with presence of small-scale magnetic structures, while in β Peg the magnetic field seems to have a more simple dipole structure. Also, in EK Boo we observe a possible decline of the magnetic activity after January 2016.

We measure a long-term trend in the radial velocity curve of EK Boo, which we think is due to the existence of a companion. We suggest that

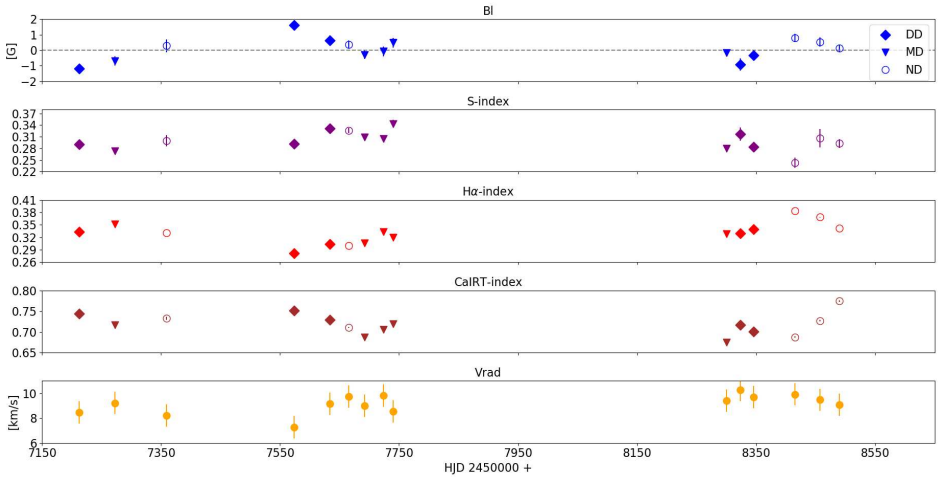

Fig. 5. Magnetic field, spectral activity indicators and radial velocity measurements of β Peg. The different symbols denote the type of detection of circular polarisation.

EK Boo is a wide binary system consisting of an M giant main component and a red dwarf companion, the latter being likely responsible for the high X-ray luminosity of the system. The magnetic variability, on the other hand, should be an intrinsic property of the main component, the giant star.

In terms of stellar evolution, β Peg and EK Boo appear at different evolutionary stages. While β Peg seems to be an early-AGB star of 3.5 solar masses (Konstantinova-Antova et al. 2014), EK Boo is of 2 or 3.6 solar masses and is respectively either at the tip RGB, or the beginning of the TP-AGB stage (Konstantinova-Antova et al. 2010). EK Boo has a larger $v\sin i$ and more magnetic field dynamics than β Peg, where the magnetic field and activity indicators behavior presume a more simple, poloidal structure. Whether an $\alpha - \omega$ dynamo or some other kind of dynamo could operate in the conditions of EK Boo remains an open question and needs a further study. An $\alpha - \omega$ dynamo seems possible in β Peg, taking into account its evolutionary stage and magnetic field behavior.

We detect a definite presence of linear polarisation in EK Boo, while in β Peg no such polarisation is found. The Stokes $U\&Q$ signal of EK Boo could in principle be caused by surface brightness inhomogeneities such as giant convective cells (similarly to the case of red supergiant stars). The existence of such giant convective cells would be in agreement with the predictions of stellar evolution theory if we consider EK Boo to be in the beginning of the TP-AGB stage. Determining the origin of net linear polarisation in this star is the aim of future works.

Acknowledgments: We thank the TBL team for proving service observing with Narval. We thank the reviewer, Dr. Stefano Bagnulo, for his valuable comments and notes. S.G., R.K.-A., R.B., A.L. and A.P. acknowledge partial support by the Bulgarian NSF project DN 18/2, including also observations in semester 2019A. R. K.-A. and A.L. acknowledge partial support under DRILA 01/3. R.K.-A. acknowledges support for the observational time in 2010 by the Bulgarian NSF project DSAB 01/2. The observations in 2008 and 2011 are under an OPTICON program. The observations in 2013 are under financial support by the OP "Human Resources Development", ESF and the Republic of Bulgaria, project BG051PO001-3.3.06-0047.

Since 2015 the Narval observations are under the French "Programme National de Physique Stellaire" (PNPS) of CNRS/INSU co-funded by CEA and CNES. N.A.D. acknowledges financial support by Russian Foundation for Basic Research (RFBR) according to the research projects 18-02-00554 and 18-52-06004. This work has made use of the VALD database, operated at Uppsala University, the Institute of Astronomy RAS in Moscow, and the University of Vienna.

References

Aurière, M. 2003, in *Magnetism and Activity of the Sun and Stars, eds. J. Arnaud, & N. Meunier, EAS Publ. Ser., 9, 105*
Aurière, M., Lòpez Ariste, A., Mathias, P., et al. 2016, *A&A, 591, A119*
Aurière, M., Konstantinova-Antova, R., Charbonnel, C., et al. 2015, *A&A, 574, A90*
Borisova, A., Aurière, M., Petit, P., et al. 2016, *A&A, 591, A57*
Charbonnel, C., Decressin, T., Lagarde, N., et al. 2017 *A&A, 605, 102*
Donati, J.-F., Semel, M., Carter, B. D., et al. 1997 *MNRAS, 291, 658*
Duncan, D. K., Vaughan, A. H., Wilson, O. C., et al. 1991, *ApJS, 76, 383*
Georgiev, S., Konstantinova-Antova, R., Borisova, A., et al. 2018, *AIP Conf. Proc., Vol. 2075, Iss. 1*
Horch, E. P., Gomez, S. C., Sherry, W. H., et al. 2011, *AJ, 141, 45*
Hünsch, M., Schmitt, J. H. M. M., Schröder, K. P., et al. 1998, *A&A, 330, 225*
Konstantinova-Antova, R., Aurière, M., Charbonnel, C., et al. 2010, *A&A, 524, A57*
Konstantinova-Antova, R., Aurière, M., Petit, P., Charbonnel, C. et al. 2012, *A&A 541, A44*
Konstantinova-Antova, R., Aurière, M., Charbonnel, C., et al. 2013, *Bulg. Astron. J., 19, 14*
Konstantinova-Antova, R., Aurière, M., Charbonnel, C., et al. 2014, in *Magnetic Fields throughout Stellar Evolution, eds. P. Petit, M, Jardine, & H. Spruit, IAUS., 302, 373*
Konstantinova-Antova, R., Lèbre, A., Aurière, M., et al. 2018, *PAS "Rudjer Bošković" No 18, 93-98*
Kupka, F., Piskunov, N., Ryabchikova, T. A., et al. 1999, *A&AS, 138, 119-133*
Lòpez Ariste, A., Mathias, P., Tessore, B., et al. 2018, *A&A, 620, A199*
Mathias, P., Aurière, M., Lòpez Ariste, A., et al. 2018, *A&A, 615, A116*
Rees, D. E., & Semel, M. D. 1979, *A&A, 74, 1*
Samus N.N., Kazarovets E.V., Durlevich O.V., et al. 2017, *GCVS 5.1, Astronomy Reports, 2017, vol. 61, No. 1, pp. 80-88*
Tabur, V., et al. 2009, *MNRAS, 400, 1945T*
Tsvetkova, S., Petit, P., Konstantinova-Antova, R., et al. 2017, *A&A, 599, A72*
van Leeuwen, F., 2007, *A&A, 474, 653V*

Appendix: Log of observations

Table 1. Log of observations in circular polarisation of EK Boo. The "$\sigma_{\rm LSD}$" column gives the RMS noise level relative to the unpolarised continuum in the LSD profiles. The "Detection" column uses the notation given in Section 2.2. The typical standard deviations of the S-, Hα- and CaIRT-index measurements are 0.007, 0.001 and 0.002 respectively. We estimate the error of our $V_{\rm rad}$ measurements to be 0.9 km/s. The dates 11jul11, 20aug11, 16jul12 and 17aug12 are affected by the Fresnel rhomb misalignment described in Section 2.3.

Date	HJD - 2450000	SNR	$\sigma_{\rm LSD}$ (10^{-5} I_c)	Exposure time	Detection	B_l [G]	σ [G]	S-index	Hα-index	CaIRT-index	$V_{\rm rad}$ [km/s]
04apr08	4562	1472	1.3	4x400s	DD	-3.38	0.74	0.242	0.356	0.648	-26.5
05apr08	4563	1358	1.4	4x400s	DD	-6.41	0.76	0.254	0.361	0.653	-26.5
06apr08	4564	1064	1.9	4x400s	DD	-6.97	1.01	0.272	0.360	0.655	-26.6
20dec08	4822	1181	1.4	6x400s	ND	0.67	0.87	0.469	0.408	0.575	-28.1
25feb09	4889	1280	1.1	8x400s	DD	-0.74	0.61	0.431	0.401	0.578	-27.5
09mar09	4900	1185	1.4	8x400s	DD	-3.84	0.53	0.420	0.392	0.575	-27.1
13mar09	4904	1401	1.2	8x400s	DD	-4.93	0.46	0.422	0.405	0.577	-27.2
18mar09	4910	904	1.3	8x400s	DD	-10.20	0.86	0.478	0.401	0.578	-27.3
18jan10	5216	601	3.3	4x400s	ND	0.28	1.59	0.413	0.372	0.579	-25.7
12feb10	5241	918	2.0	8x400s	ND	0.28	1.01	0.296	0.393	0.641	-24.8
13mar10	5270	1097	1.4	8x400s	MD	1.48	0.70	0.322	0.393	0.630	-24.5
15apr10	5303	1281	1.2	8x400s	MD	-0.80	0.61	0.302	0.376	0.632	-25.2
23apr10	5311	1269	1.3	8x400s	ND	-0.44	0.68	0.281	0.382	0.657	-24.3
22jun10	5370	1223	1.3	8x600s	ND	0.34	0.67	0.297	0.379	0.657	-23.2
07jul10	5385	1177	1.1	8x400s	MD	1.76	0.63	0.270	0.384	0.617	-25.4
23jul10	5401	1133	1.3	8x400s	ND	1.64	0.66	0.296	0.393	0.656	-24.6
17aug10	5426	1095	1.5	8x400s	ND	0.67	0.78	0.278	0.407	0.684	-23.3
13jan11	5576	721	2.0	8x400s	ND	0.70	1.20	0.316	0.416	0.672	-24.0
15jan11	5578	1187	1.1	8x400s	ND	0.25	0.73	0.287	0.415	0.667	-23.8
04feb11	5598	1412	1.0	8x400s	ND	0.67	0.57	0.259	0.402	0.657	-24.0
18mar11	5640	1015	1.4	8x400s	ND	0.58	0.84	0.303	0.388	0.641	-25.4
31mar11	5653	763	1.9	8x400s	ND	2.71	1.05	0.325	0.399	0.678	-24.6
07apr11	5660	1171	1.2	8x400s	DD	3.25	0.69	0.313	0.395	0.672	-24.4
30apr11	5683	963	1.5	8x400s	ND	3.89	0.83	0.319	0.369	0.611	-25.7
12may11	5695	1386	1.0	9x400s	ND	1.13	0.55	0.303	0.361	0.597	-25.9
13jun11	5726	1196	1.2	8x400s	ND	-0.15	0.69	0.307	0.363	0.619	-25.8
01jul11	5744	1223	1.2	8x400s	ND	-0.66	0.67	0.309	0.357	0.597	-25.9
11jul11	5754	1243	1.1	8x400s	N/A	N/A	N/A	0.316	0.351	0.604	-25.6
20aug11	5794	1167	1.2	8x400s	N/A	N/A	N/A	0.296	0.337	0.583	-26.5
07jan12	5935	1332	1.2	8x400s	DD	4.93	0.71	0.320	0.326	0.604	-24.8
24jan12	5952	1290	1.1	8x400s	MD	2.89	0.66	0.320	0.341	0.612	-24.5
13mar12	6001	1286	1.2	8x400s	ND	-0.31	0.67	0.344	0.361	0.642	-23.5
09may12	6058	799	2.0	8x400s	ND	-0.94	1.10	0.333	0.376	0.658	-23.1
14jun12	6094	754	2.2	8x400s	ND	-1.94	1.13	0.301	0.349	0.607	-23.9
16jul12	6125	1243	1.2	8x400s	N/A	N/A	N/A	0.259	0.368	0.652	-23.1
17aug12	6157	1031	1.4	8x400s	N/A	N/A	N/A	0.253	0.355	0.585	-24.2
21mar13	6374	839	2.6	4x400s	DD	-8.12	1.51	0.281	0.354	0.645	-25.1
21apr13	6405	1011	1.9	4x400s	DD	-4.96	1.14	0.276	0.350	0.593	-24.0
10jun13	6454	891	2.4	4x400s	ND	1.00	1.35	0.262	0.371	0.653	-22.4
11aug13	6516	1288	1.6	4x400s	MD	-3.34	0.91	0.224	0.366	0.624	-23.9
24jan16	7413	968	2.3	4x400s	ND	-0.10	1.30	0.284	0.389	0.628	-21.9
16feb16	7436	1185	1.3	8x400s	ND	0.07	0.77	0.263	0.399	0.615	-21.8
16mar16	7465	1025	1.5	8x400s	ND	-2.48	0.82	0.259	0.395	0.614	-21.8
13apr18	8223	564	3.3	7x400s	ND	-1.75	1.70	0.287	0.360	0.590	-23.7
05may18	8244	1001	1.6	8x400s	ND	-0.46	0.89	0.228	0.374	0.612	-21.7
14jun18	8284	1153	1.3	8x400s	ND	-0.79	0.65	0.209	0.381	0.559	-21.8
17jul18	8317	1233	1.3	8x400s	MD	-0.86	0.63	0.202	0.388	0.578	-21.7
07aug18	8338	906	1.8	8x400s	ND	-1.59	1.03	0.224	0.390	0.612	-20.7
27aug18	8358	980	1.7	8x400s	ND	-1.62	0.94	0.246	0.382	0.588	-21.2
14jan19	8499	1088	1.5	8x400s	ND	-0.14	0.89	0.232	0.392	0.683	-21.1
19apr19	8594	882	1.8	8x400s	MD	1.22	1.02	0.214	0.374	0.660	-22.8

Table 2. Log of observations in circular polarisation of β Peg. The "$\sigma_{\rm LSD}$" column gives the RMS noise level relative to the unpolarised continuum in the LSD profiles. The "Detection" column uses the notation given in Section 2.2. The typical standard deviations of the S-, Hα- and CaIRT-index measurements are 0.009, 0.001 and 0.002 respectively. We estimate the error of our $V_{\rm rad}$ measurements to be 0.9 km/s.

Date	HJD - 2450000	SNR	$\sigma_{\rm LSD}$ ($10^{-5} I_c$)	Exposure time	Detection	B_l [G]	σ [G]	S-index	Hα-index	CaIRT-index	$V_{\rm rad}$ [km/s]
08jul15	7213	1683	0.7	8x80s	DD	-1.17	0.22	0.291	0.333	0.744	8.5
06sep15	7273	1138	1.0	8x70s	MD	-0.69	0.29	0.274	0.351	0.716	9.2
02dec15	7359	798	1.3	8x70s	ND	0.29	0.41	0.299	0.331	0.733	8.2
03jul16	7574	1604	0.7	8x70s	DD	1.62	0.22	0.292	0.281	0.752	7.3
01sep16	7633	1271	0.9	8x70s	DD	0.64	0.31	0.331	0.303	0.729	9.2
03oct16	7665	1317	0.9	8x70s	ND	0.37	0.27	0.326	0.300	0.710	9.7
30oct16	7692	1294	0.9	8x70s	MD	-0.28	0.27	0.309	0.306	0.687	9.1
01dec16	7724	1155	1.0	8x70s	MD	-0.08	0.31	0.304	0.333	0.706	9.8
17dec16	7740	1049	0.9	8x70s	MD	0.48	0.30	0.344	0.319	0.720	8.5
30jun18	8301	1361	0.9	8x80s	MD	-0.16	0.24	0.280	0.328	0.674	9.4
23jul18	8324	1062	1.2	8x80s	DD	-0.92	0.39	0.317	0.329	0.717	10.3
14aug18	8346	1477	0.7	8x80s	DD	-0.32	0.26	0.283	0.339	0.701	9.7
23oct18	8416	1388	0.9	8x80s	ND	0.78	0.26	0.243	0.384	0.688	9.9
04dec18	8457	1188	1.1	7x80s	ND	0.54	0.30	0.306	0.368	0.727	9.5
06jan19	8490	1597	0.8	8x80s	ND	0.14	0.23	0.293	0.342	0.774	9.1